Energy 35 (2010) 1200–1210

Contents lists available at ScienceDirect

Energy

journal homepage: www.elsevier.com/locate/energy

COOLCEP (cool clean efficient power): A novel CO_2-capturing oxy-fuel power system with LNG (liquefied natural gas) coldness energy utilization☆

Na Zhang [a,*], Noam Lior [b], Meng Liu [c], Wei Han [a]

[a] Institute of Engineering Thermophysics, Chinese Academy of Sciences, Beijing 100190, PR China
[b] Department of Mechanical Engineering and Applied Mechanics, University of Pennsylvania, Philadelphia, PA 19104-6315, USA
[c] Division of Research and Environment Standardization, China National Institute of Standardization, Beijing 100080, PR China

ARTICLE INFO

Article history:
Received 22 October 2008
Received in revised form
12 February 2009
Accepted 1 April 2009
Available online 13 May 2009

Keywords:
Oxy-fuel power system
LNG
Coldness energy
Power generation
CO_2 capture

ABSTRACT

A novel liquefied natural gas (LNG) fueled power plant is proposed, which has virtually zero CO_2 and other emissions and a high efficiency. The plant operates as a subcritical CO_2 Rankine-like cycle. Beside the power generation, the system provides refrigeration in the CO_2 subcritical evaporation process, thus it is a cogeneration system with two valued products. By coupling with the LNG evaporation system as the cycle cold sink, the cycle condensation process can be achieved at a temperature much lower than ambient, and high-pressure liquid CO_2 can be withdrawn from the cycle without consuming additional power. Two system variants are analyzed and compared, COOLCEP-S and COOLCEP-C. In the COOLCEP-S cycle configuration, the working fluid in the main turbine expands only to the CO_2 condensation pressure; in the COOLCEP-C cycle configuration, the turbine working fluid expands to a much lower pressure (near-ambient) to produce more power. The effects of some key parameters, the turbine inlet temperature and the backpressure, on the systems' performance are investigated. It was found that at the turbine inlet temperature of 900 °C, the energy efficiency of the COOLCEP-S system reaches 59%, which is higher than the 52% of the COOLCEP-C one. The capital investment cost of the economically optimized plant is estimated to be about 750 EUR/kWe and the payback period is about 8–9 years including the construction period, and the cost of electricity is estimated to be 0.031–0.034 EUR/kWh.

1. Introduction

Liquefied natural gas (LNG) has a temperature of about 110 K, much lower than that of the ambient air or water, and thus preserves a large amount of coldness exergy. At the receiving terminals, instead of simply providing the heat for the LNG evaporation process from ambient seawater or air, as is often done in practice, and thus wasting the valuable coldness, it is possible to withdraw the coldness exergy from the LNG evaporation process by investing it in some process which recovers it for some useful application. One way to achieve this is by incorporating it into a properly designed thermal power cycle that uses the LNG evaporator as its cold sink [1–11].

Use of the coldness energy of LNG for power generation includes methods which use the LNG as the working fluid in natural gas direct expansion cycles, or its coldness as the heat sink in closed-loop Rankine cycles [1–6], Brayton cycles [7,8], and combinations thereof [9,10]. Other methods use the LNG coldness to improve the performance of conventional thermal power cycles. For example, LNG vaporization can be integrated with steam turbine condenser system (by cooling the recycled water [10]) or gas turbine inlet air cooling [11], etc.

In addition to improving power generation system efficiency, we are addressing in this work also the need for CO_2 capture, which is energy consuming and decrease power generation efficiency, and also increase its cost [12,13].

One of the proposed CO_2 capture strategies involves oxy-fuel combustion. It is based on close-to-stoichiometric combustion of the fuel with enriched oxygen (produced in an air separation unit, ASU) in the presence of recycled flue gas. Avoiding the use of air as the oxygen source in the combustor, the advantage of oxy-fuel combustion is that it thus takes place in the absence of the large amounts of nitrogen, and produces only CO_2 and H_2O. The water is condensed out of this mixture, leaving the CO_2 separated, and this separation process therefore requires only a modest amount of energy.

Some oxy-fuel cycles with ASU and recycled CO_2/H_2O from the flue gas are the Graz cycle, Water cycle and Matiant cycle [14–19].

☆ Patent pending.

* Corresponding author. Tel.: +86 10 82543030; fax: +86 10 82543019.
E-mail address: zhangna@mail.etp.ac.cn (N. Zhang).

0360-5442/$ – see front matter © 2009 Elsevier Ltd. All rights reserved.
doi:10.1016/j.energy.2009.04.002

Nomenclature

A	area [m^2]
C_{CO_2}	the annual CO_2 credit [10^6 EUR]
C_f	the annual fuel cost [10^6 EUR]
C_i	the total plant investment [10^6 EUR]
C_m	the annual O&M cost [10^6 EUR]
C_P	specific heat [kJ/kg K]
COE	cost of electricity [EUR/kWh]
e	specific exergy [kJ/kg]
E_C	total refrigeration exergy output [MW]
H	the annual operation hours [h]
LHV	lower heating value of fuel [kJ/kg]
m	mass flow rate [kg/s]
n	the plant operation life [year]
p	pressure [bar]
p_b	backpressure [bar]
Q	heat [kW]
Q_c	refrigeration [kW]
R	ratio of net power output to refrigeration exergy
R_{CO_2}	CO_2 recovery ratio
s	specific entropy [kJ/kg K]
St	Stanton number
T	temperature [°C]
TIT	turbine inlet temperature [°C]
TOT	turbine outlet temperature [°C]
W_{net}	net power output (after deducting also the ASU power consumption) [MW]
W_{sp}	specific power output [kJ/kg]
η_c	blade cooling efficiency [%]
β	coefficient, Eq. (5)
η_e	power generation efficiency [%], Eq. (1)
ε	exergy efficiency [%], Eq. (2)
ε_c	cooling effectiveness
δ_f	film cooling effectiveness

Subscripts

b	blade
c	cooling, coolant
f	fuel
g	gas
LNG	liquefied natural gas
wf	working fluid
1,2…23	states on the cycle flowsheet

Abbreviations

ASU	air separation unit
BOP	balance of plant
C	compressor
COM	combustor
CON	condenser
EVA	evaporator
GT	Gas Turbine
HEX	heat exchanger
LNG	liquefied natural gas
NG	natural gas
P	Pump
REP	recuperator

We proposed and analyzed the semi-closed oxy-fuel cycles with integration of the LNG cold exergy utilization [20,21]. The additional power use for O_2 production amounts to 7–10% of the cycle's total input energy. To reduce the oxygen production efficiency penalty, new technologies have been developed, such as chemical looping combustion (CLC) [22,23] and the AZEP concept [24], employing oxygen transport particles and membranes to separate O_2 from air. Kvamsdal et al. [25] made a quantitative comparison of various cycles with respect to plant efficiency and CO_2 emissions, and concluded that the adoption of these new technologies shows promising performance because no additional energy is then necessary for oxygen separation, but they are still under development.

In this paper we present, model, and compare two configurations of a novel power generation system family with LNG cold energy utilization and CO_2 capture, that we named COOLCEP[1] (Cool Clean Efficient Power). They generate power and produce refrigeration if needed, evaporate LNG (and thus convert the LNG cold for power generation), and capture the combustion-generated CO_2. These systems have both high power generation efficiency and extremely low environmental impact.

2. System configuration description

- COOLCEP-S, which is based on the concept proposed by Deng et al. [6] and is a cogeneration (power and refrigeration) recuperative Rankine cycle with CO_2 as the main working fluid, the working fluid in the main turbine expands only to the CO_2 condensation pressure.
- COOLCEP-C, which is a variation of the COOLCEP-S cycle but with a lower turbine backpressure (near-ambient) to produce more power. In addition, the turbine exhaust temperature, and therefore the regenerator hot stream inlet temperature are at a lower level, eliminating the need for the higher temperature heat exchanger. However, it then requires a compressor to raise the CO_2 pressure to the condensation level.

2.1. The COOLCEP-C configuration

Fig. 1 shows the layout of the COOLCEP-C cycle, which consists of a power subcycle and an LNG vaporization process. Fig. 2 is the

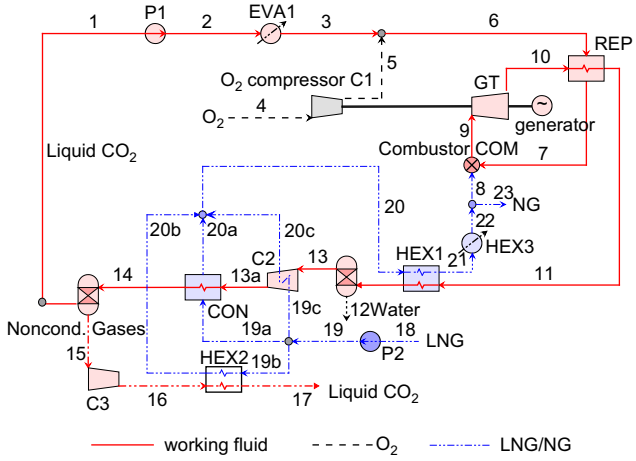

Fig. 1. The process flowsheet of the COOLCEP-C system.

[1] Patent pending.

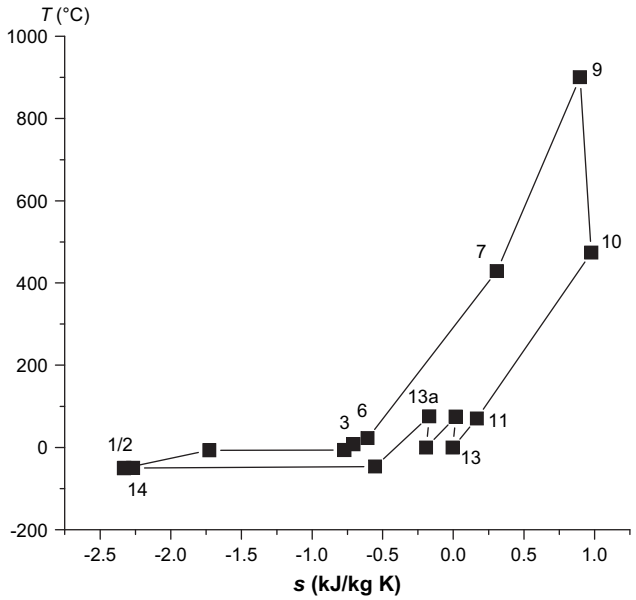

Fig. 2. Cycle *T*–*s* diagram in the COOLCEP-C system.

cycle *T*–*s* diagram. The interfaces between the power subcycle and the LNG vaporization process are the CO_2 condenser CON, the heat exchanger HEX1 and the fuel feed stream 8.

The power subcycle can be identified as 1–2–3–4–5–6–7–8–9–10–11–12/13–13a–14–1. The low temperature (−50 °C) liquid CO_2 as the main working fluid (1) is pumped to about 30 bar (2), then goes through a heat addition process (2–3) in the evaporator EVA1 and can thereby produce refrigeration if needed. The O_2 (4) produced in an air separation unit (ASU) is compressed and mixed with the main CO_2 working fluid. The gas mixture (6) is heated (6–7) by turbine (GT) exhaust heat recuperation in REP. The working fluid temperature is further elevated in the combustor COM, fueled with natural gas (8), to its maximal value (the turbine inlet temperature *TIT*) (9). The working fluid expands to near-ambient pressure (10) in the gas turbine (GT) to generate power and is then cooled (to 11) in the recuperator REP.

The gases in the mixture at the exit of REP (11) need to be separated, and the combustion-generated CO_2 component needs to be condensed for ultimate sequestration, and this is performed by further cooling in the LNG-cooled heat exchanger HEX1, in which the H_2O vapor in the mixture is condensed and drained out (12). Afterwards, the remaining working gas (13) is compressed to the condensation pressure (13a), and one stage inter-cooling (19c–20c) is adopted in the compressor to reduce the compression work. The CO_2 working fluid is condensed (14) in the condenser CON against the LNG evaporation, and recycled (1). The remaining working fluid (15) enriched with noncondensable species (mainly N_2, O_2 and Ar) is further compressed in C3 to a higher pressure level under which the combustion-generated CO_2 is condensed and captured, ready for final disposal.

The LNG vaporization process is 18–19–19a/b/c–20a/b/c–20–21–22–23/8. LNG (18) is pumped by P2 to the highest pressure (73.5 bar), typical for receiving terminals which supply long distance pipeline network, and then evaporated with the heat addition from the power cycle. The evaporated NG (natural gas) may produce a small amount of cooling in HEX3 if its temperature is still low enough at the exit of HEX1, and thus contribute to the overall system useful outputs. Finally, the emerging natural gas stream is split into two parts where most of it (23) is sent to outside users and a small part (8) is used as the fuel in the combustor.

In this configuration, a compressor C2 is required to raise the expanded CO_2 gas (13) pressure to the condensation level, with the associated efficiency penalty due to the energy consumption of the compressor.

2.2. The COOLCEP-S configuration

Noting from preliminary analysis that the necessity for the gas compressor in system COOLCEP-C (process 13–13a in Figs. 1 and 2) consumes a significant amount of power for the pressure elevation, system COOLCEP-S was configured so that the working fluid expands in the turbine GT to only the working fluid condensation pressure, at the expense of some amount of power generation in the turbine, thus eliminating the need for this gas compression process. Its *T*–*s* diagram is shown in Fig. 3. As a result, the turbine in COOLCEP-S has a higher backpressure compared with that in COOLCEP-C and its exhaust is at a higher temperature (the regenerator REP hot stream inlet temperature). It is noted that the higher temperature in heat exchanger REP requires special attention to its design. The working fluid pressure elevation is accomplished entirely by the much less energy consuming process of pressurizing a liquid (process 1–2 in Fig. 1).

COOLCEP-S basically follows the cycle concept proposed in Ref. [6] but with a different condensation process: first the amount of the working fluid needed for sustaining the process is condensed and recycled; and then the remaining working fluid, having a relatively small mass flow rate (<5% of the total turbine exhaust flow rate after water removal) and higher concentration of noncondensable gases, is compressed to a higher pressure level and then condensed. Alternatively, the CO_2-enriched flue gas can be condensed at a lower temperature, which can be provided by the LNG coldness, but it would then freeze the CO_2 and is thus not considered in this paper; instead we adopted a higher condensation pressure for the flue stream condensation, which leads to a more conservative solution and some efficiency penalty but can recover the CO_2 fully.

3. Calculation assumptions

The simulations were carried out using the commercial Aspen Plus software [26], in which the component models are based on the energy balance and mass balance, with the default relative

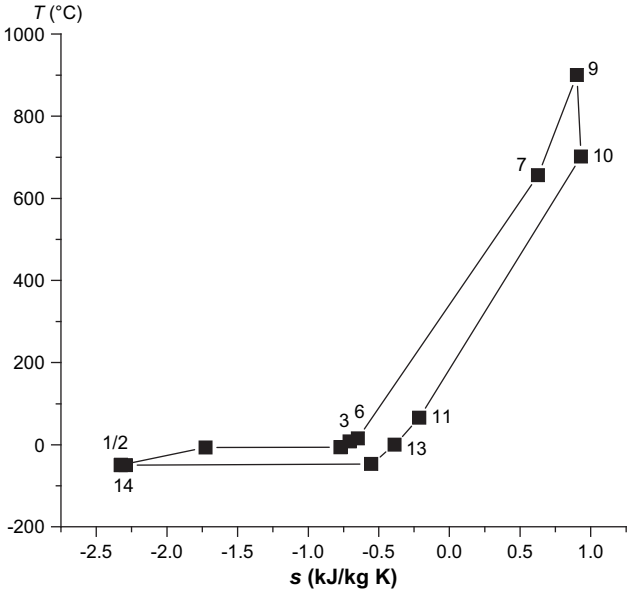

Fig. 3. Cycle *T*–*s* diagram in the COOCEP-S system.

convergence error tolerance of 0.01%. The PSRK property method was selected for the thermal property calculations. It is based on the Predictive Soave–Redlich–Kwong equation-of-state model, which is an extension of the Redlich–Kwong–Soave equation of state. It can be used for mixtures of non-polar and polar compounds, in combination with light gases, and up to high temperatures and pressures.

Some properties of the feed streams are reported in Table 1. 95 mol% oxygen from a cryogenic ASU is chosen for the combustion, since this was considered to be the optimal oxygen purity when taking into account the tradeoff between the cost of producing the higher-purity oxygen and the cost of removing noncondensable species from the CO_2 [27]. The O_2 composition and its power consumption for production follow those in Ref. [25]. Some other assumptions for the calculation are summarized in Table 2.

The commonly used thermal power generation efficiency is defined as:

$$\eta_e = W_{net}/\left(m_f \cdot LHV\right) \quad (1)$$

Since the power and refrigeration cogeneration energy efficiency definition is somewhat problematic (cf. [28]), for evaluating the cogeneration we define the exergy efficiency as:

$$\varepsilon = (W_{net} + E_c)/\left(m_f e_f + m_{LNG} e_{LNG}\right) \quad (2)$$

with both the power and cooling as the outputs, and both the fuel exergy and LNG cold exergy as the inputs. The cooling rate exergy E_C is the sum of the refrigeration exergy produced in the evaporators EVA1 and HEX3. In the calculation below, the processed LNG mass flow rate is chosen to be the least which can sustain the cooling demand of the power cycle exothermic process.

The CO_2 recovery ratio is defined as:

$$R_{CO_2} = m_{R,CO_2}/m_{COM,CO_2} \quad (3)$$

where m_{COM,CO_2} is the combustion-generated CO_2, and m_{R,CO_2} is the mass flow rate of the liquid CO_2 in stream (17) (Fig. 1) that is retrieved.

The turbine inlet temperature *TIT* is a key parameter for the system performance, generally the higher the *TIT*, the higher the system efficiency. However, higher turbine inlet temperature always requires advanced combustors and turbine blade design and cooling, and also advanced materials, and thus raises the gas turbine cost.

The adoption of blade cooling in gas turbine systems generally allows higher *TIT* and therefore higher performance gain. However, it has also some negative influence on the gas turbine performance because 1) extraction of the coolant gas from the working fluid decreases the working fluid mass flow rate for power generation; 2) its mixing with the main gas reduces the local gas temperature and pressure, leading to further loss of power generation; and 3) in a recuperative gas turbine cycle, the gas turbine exhaust temperature decreases and less exhaust heat is therefore available for recuperation, leading to drop of the combustor working fluid inlet temperature and consequently to a higher fuel demand. With the conventional blade cooling technology, such as the convective or film cooling, the efficiency increases at a diminishing rate with the increase of *TIT* because higher *TIT* requires a higher blade coolant flow extraction. As *TIT* is raised, there is point at which the gain from the increase of *TIT* will be offset by these negative effects of blade cooling application. At *TIT* values higher than this, the gas turbine efficiency drops. Therefore more advanced cooling technologies such as transpiration cooling or close-loop steam cooling are developed for advanced gas turbines. The performance with and without turbine cooling consideration is compared below. A description of the turbine blade cooling model is given in the Appendix.

Table 1
Molar composition and some properties for feed streams.

	LNG	O_2
CH_4 [mol %]	90.82	
C_2H_6 [mol %]	4.97	
C_3H_8 [mol %]	2.93	
C_4H_{10}	1.01	
N_2 [mol %]	0.27	2
O_2 [mol %]		95
Ar [mol %]		3
Temperature [°C]	−161.5	25
Pressure [bar]	1.013	2.38
Lower heating value [kJ/kg]	49,200	–
Specific exergy [kJ/kg]	50,950	
Power consumption for O_2 production [kJ/kg]		812

Table 2
Main assumptions for the calculation.

Ambient state	Temperature [°C]	25
	Pressure [bar]	1.013
Combustor	Pressure loss [%]	3
	Efficiency [%]	100
	Excess O_2 beyond the stoichiometric ratio [%]	2
Turbine	Isentropic efficiency [%]	90
Recuperator	Pressure loss [%]	3
	Minimal temperature difference [°C]	45
LNG vaporization unit	Pressure loss [%]	3
	Temperature difference at pinch point [°C]	8
CO_2 condenser	Condensation pressure [bar]	7
	Condensation temperature [°C]	−50
Pump efficiency [%]		80
Compressor efficiency [%]		88
(Mechanical efficiency) × (generator electrical efficiency) [%]		96

To avoid CO_2 freezing, the condensation pressure is kept above the triple point pressure of 5.18 bar, and the temperature is chosen to be above −50 °C. The simulation has shown that at the condensation pressure of 7 bar, the mass flow rate of the condensed CO_2 is merely sufficient for the working fluid recycling; and that the condensed CO_2 flow rate increases as the condensation pressure increases. The higher condensation pressure, however, requires more compressor work, resulting in lower system efficiency. Considering the significant influence of the condensation pressure on both system thermal performance and the CO_2 recovery, the working fluid is compressed to 7 bar, and then the CO_2 is condensed for recycling as the working fluid. Only the remaining uncondensed working fluid that has a mass flow rate of only 2–5% of the total turbine exhaust after water removal, and high concentration of noncondensable species (the composition is about 88 mol% CO_2, and ~12 mol% of the noncondensable gases N_2, O_2 and Ar) will thus be compressed to a higher pressure for the CO_2 condensation and recovery.

In the COOLCEP-C system, a CO_2 compressor is incorporated to elevate the working fluid pressure for CO_2 condensation. To take advantage of the LNG coldness and to reduce the compressor power consumption, the compressor inlet stream should be cooled to the lowest possible temperature. However, to eliminate the technological difficulty associated with the low inlet temperature compressor, we assumed in this study that the turbine exhaust gas is cooled in HEX1 just to 0 °C. Water is condensed and removed before CO_2 compression in C2. A trace amount of CO_2 will in any case be dissolved in the water and be removed along with it. To simplify the simulation it is assumed that water and CO_2 are fully separated.

A parametric analysis is conducted to investigate the influence of key parameters, which are the turbine inlet temperature and the turbine backpressure. Based on these analyses, the parameters are chosen and the two configurations are compared.

4. Parametric sensitivity analysis

4.1. Investigation on the influence of the turbine inlet temperature *TIT*

We vary the *TIT* from 900 °C to 1250 °C and the two cases with or without considering gas turbine blade cooling are investigated and compared. While blade cooling is mandatory at high *TIT*, but this analysis was performed over the entire *TIT* range even without cooling, just to show the influence of the blade cooling and the errors if its effect has been ignored, and help to choose an optimal *TIT* value under different conditions. The parameters examined are the specific power output W_{sp}, the fuel mass flow m_f, the cycle thermal efficiency η_e and the cogeneration exergy efficiency ε. The parameters listed in Table 2 are kept constant in the sensitivity analysis.

Fig. 4 shows that the increasing turbine inlet temperature *TIT* increases the specific power output W_{sp}, as well as the extent to which turbine blade cooling reduces W_{sp}. Obviously the blade cooling has bigger influence at higher *TIT* because of the higher demand of cooling stream extraction. The COOLCEP-C system has a much higher W_{sp} than COOLCEP-S, because the turbine in the former expands to a much lower backpressure.

The effect of *TIT* on the cycle power generation efficiency η_e is shown in Fig. 5. When blade cooling effect is considered, the energy efficiency exhibits a maximum, because increasing *TIT* demands a higher blade coolant flow rate, and thus a point is reached at which the gain from the increase of *TIT* will be offset by thermodynamically negative effects of blade coolant application. For the COOLCEP-C cycle, the *TIT* at which the power generation efficiency has a maximum, of 54.1%, is about 1200 °C; and for the COOLCEP-S system the maximal power generation efficiency, of 58.6%, is at the much lower *TIT* of ~900 °C. At *TIT* < 1170 °C, the COOLCEP-S system has higher power generation efficiency than COOLCEP-C, but drops quickly below it as *TIT* increases. If the blade cooling effect is not considered, the power generation efficiency exhibits a monotonic

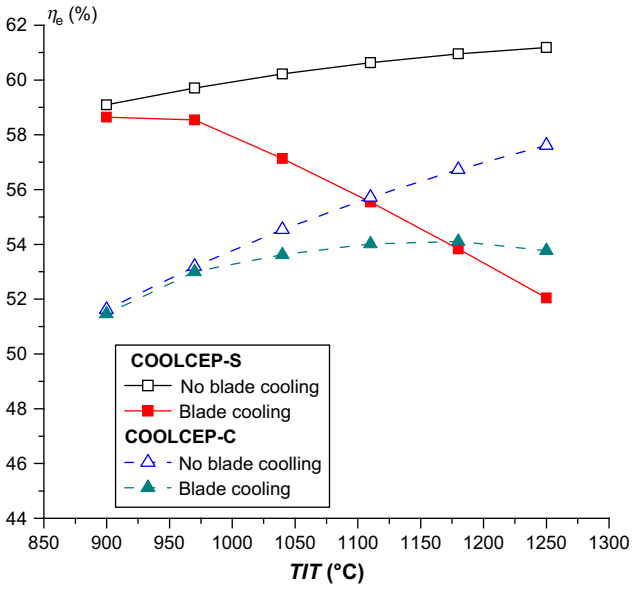

Fig. 5. The power generation efficiency η_e vs. *TIT*.

increase with increasing *TIT*, COOLCEP-S system has a higher efficiency than that of the COOLCEP-C system, especially in the lower *TIT* region. For example, when *TIT* = 900 °C and without considering blade cooling effect, the power generation efficiency for COOLCEP-S is 59.1%, higher by 7.4%-points than that for COOLCEP-C. The lower efficiency of COOLCEP-C system is because of higher specific fuel consumption. Though it produces more specific power generation, the specific fuel consumption is double in the COOLCEP-C than that in the COOLCEP-S system (as shown in Fig. 6), because the turbine exhausts at a much lower temperature in COOLCEP-C, making less heat available for recuperation and therefore creating a larger fuel demand elevating the working fluid temperature after the recuperation in REP.

It is also noted that blade cooling has bigger effect on power efficiency than on specific power output, this is because the proposed system configurations are recuperative gas turbine cycles,

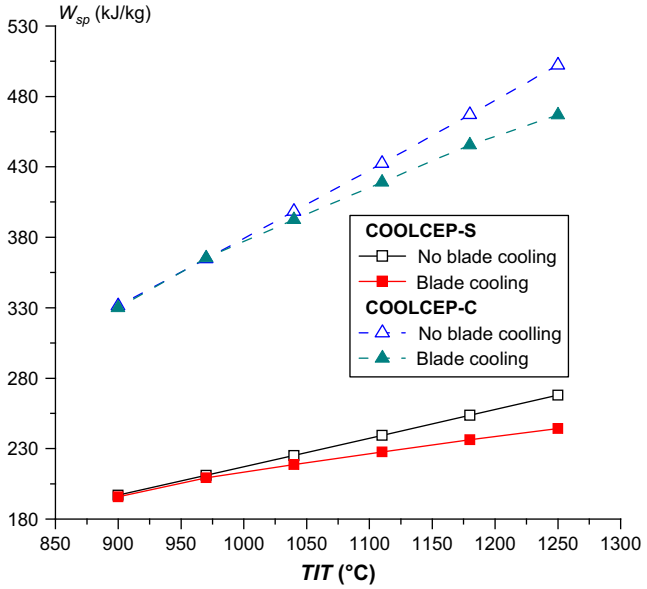

Fig. 4. The specific power output W_{sp} vs. *TIT*.

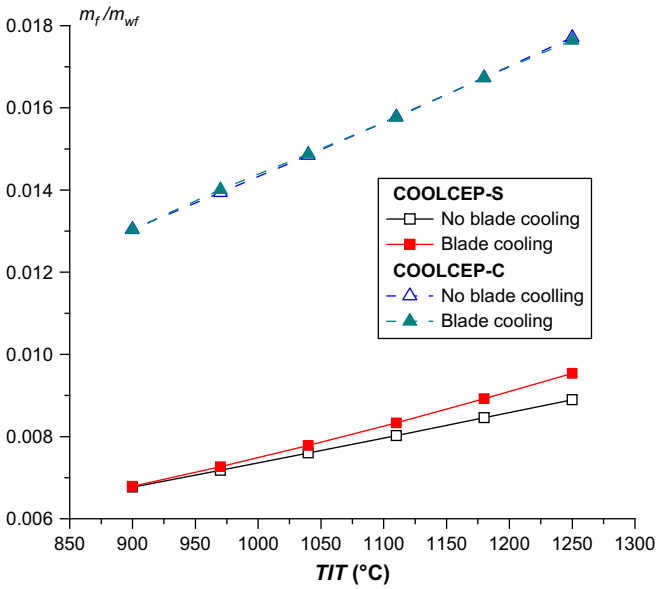

Fig. 6. The fuel mass flow rate m_f vs. *TIT*.

and the hot-end heat transfer temperature difference in REP is kept constant in the calculation while *TIT* is varied. As stated before, beside the thermodynamic performance impairment by the blade cooling due to working fluid extraction and its temperature/pressure reduction, in a recuperative gas turbine cycle the gas turbine exhaust temperature decreases and less exhaust heat is therefore available for recuperation, leading to a drop of the combustor working fluid inlet temperature and consequently to a higher fuel demand, while the drop of the recuperative heat doesn't affect the specific power output. Blade cooling therefore causes a higher efficiency penalty in a recuperative gas turbine cycle than in a simple gas turbine cycle, but its effects on the specific power output are the same.

The cogeneration exergy efficiency, which accounts for both power and cooling outputs, is shown in Fig. 7. It has similar variation tendency with *TIT* as there is also a value of *TIT* that maximizes the efficiency when blade cooling effect is considered. Without blade cooling consideration, the COOLCEP-S system has better performance in the lower *TIT* region, the exergy efficiency ε is 39.8% for *TIT* = 900 °C. The COOLCEP-C system has higher ε in the higher *TIT* region.

The conclusions from this analysis with and without considering turbine blade cooling are that the effect of the turbine blade cooling may have some influence on the system performance, and its effect should not be ignored especially in the high *TIT* region. It is suggested that advanced cooling technology, such as transpiration or closed-loop steam cooling, should be employed in the higher *TIT* region instead of the conventional convective and film cooling considered in this analysis. For the COOLCEP-S system which has a higher backpressure, the higher *TIT* values are thus undesirable because they both reduce the efficiency and raise the turbine system cost. In the analysis below, the turbine with a *TIT* of ~900 °C and without blade cooling is investigated further, assuming 900 °C is the highest limit for a gas turbine without blade cooling.

4.2. Investigation on the influence of turbine backpressure p_b

In the calculation below, the turbine inlet temperature *TIT* is fixed at 900 °C and blade cooling is not employed. The calculation region can be divided into two:

1) for $p_b < 7.1$ bar, the system configuration is the COOLCEP-C, in which the CO_2 condensation pressure remains unchanged at 7 bar as p_b is varied from 1.1 bar to 7.1 bar.
2) for $p_b \geq 7.1$ bar, the CO_2 compression before condensation is not necessary anymore, the system configuration is the COOLCEP-S, in which the CO_2 condensation pressure varies with the value of p_b.

Fig. 8 shows the variation of the system specific power output with p_b. Though the increase of p_b reduces the power consumption of the CO_2 compressor C2, it has a more significantly negative effect on the turbine power output, leading to the drop of the net power output. In the investigated range, the highest specific power output of 330 kJ/kg is found for the COOLCEP-C system with p_b of 1.1 bar. For the COOLCEP-S system with the backpressure of 7.1 bar, the specific power output is about 197 kJ/kg. More importantly, this value is comparable or even higher than the specific power output of commercial gas turbines with the same *TIT* value of 900 °C.

Fig. 9 shows that raising p_b decreases the required fuel mass flow m_f. This is because the increasing turbine exits temperature that accompanies the increase of turbine backpressure makes more heat available for recuperation, thus reducing the fuel demand in the combustor.

Fig. 10 shows the variation of the power generation efficiency with p_b. For $p_b < 7.1$ bar, the system configuration is the COOLCEP-C. Raising p_b increases the thermal efficiency η_e from 51.6% (at $p_b = 1.1$ bar) to 59% (at $p_b = 7.1$ bar). This is mainly because raising p_b decreases the required fuel mass flow m_f. In the region $p_b \geq 7.1$ bar the system changes to the COOLCEP-S configuration, and increasing p_b beyond 7.1 bar decrease the efficiency. This is because both the turbine power generation and the fuel demand drop as the backpressure increases, but the drop of the turbine power output dominates in this case. The exergy efficiency ε undergoes a similar trend of rising from 37.3% (at $p_b = 1.1$ bar) to 39.8% (at $p_b = 7.1$ bar) and then decreasing for $p_b \geq 7.1$ bar.

The results suggest that although increase of the turbine backpressure p_b causes a decrease in the net power output, it raises the cycle thermal efficiency η_e and the exergy efficiency ε as long as p_b is lower than the CO_2 condensation pressure. Both cycle efficiencies reach a maximum when p_b is increased to the CO_2 condensation pressure, at which point the need for CO_2 compression before its

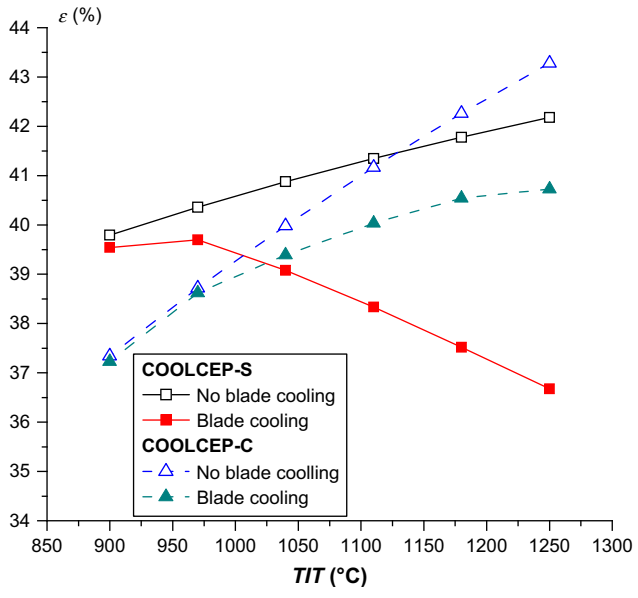

Fig. 7. The cogeneration exergy efficiency ε vs. *TIT*.

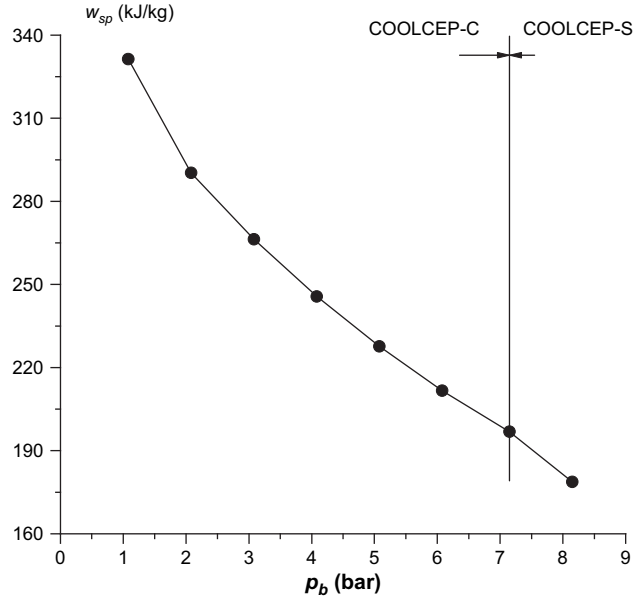

Fig. 8. The specific power output W_{sp} vs. p_b.

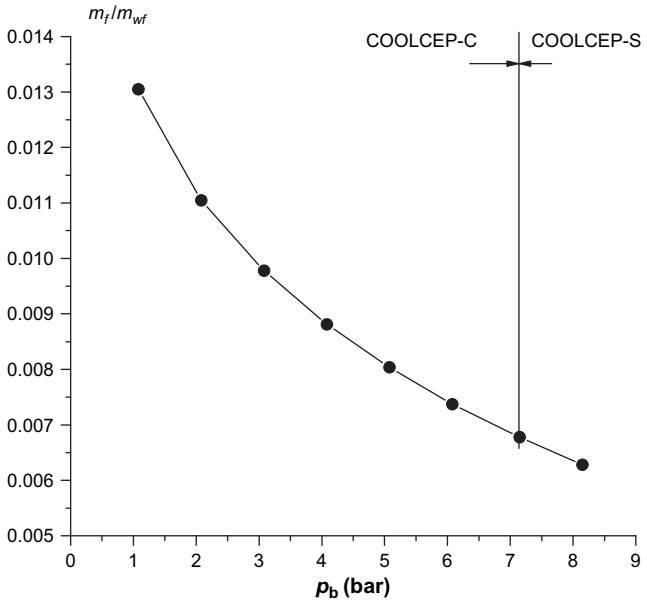

Fig. 9. The fuel mass flow rate m_f vs. p_b.

condensation is eliminated, and thus the system changes to the COOLCEP-S configuration, which has a lower specific power output, but is more efficient and simpler.

The turbine exhaust temperature (*TOT*) increases as p_b is increased, but it remains below 701 °C for $p_b \leq 7.1$ bar due to our choice of the relatively low *TIT* of 900 °C. With this lower temperature of the recuperator REP inlet hot stream (10), the heat exchanger becomes more conventional, with a much lower price and much higher commercial availability.

5. Comparison between the two systems

To generate the same net power output W_{net} of 20 MW, Table 3 summarizes the cycle performance with *TIT* fixed at 900 °C. Tables 4 and 5 report the major stream parameters of the main state points of the two systems.

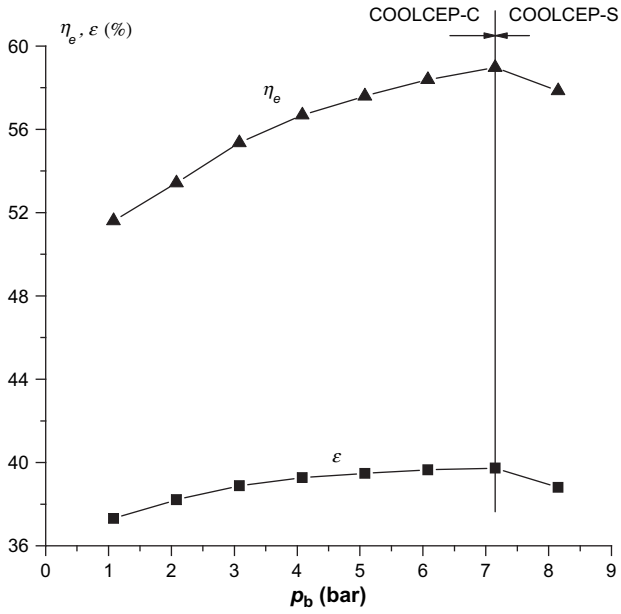

Fig. 10. The efficiencies η_e and ε vs. p_b.

1) Specific power output: the COOLCEP-C has a higher specific power output

   In the COOLCEP-C system, the lower turbine backpressure p_b leads to much higher turbine work output and specific power output W_{sp} than those in the COOLCEP-S: the specific power output of 331 kJ/kg in COOLCEP-C system is 68% higher than the 197 kJ/kg in the COOLCEP-S system. 24% of the turbine power output W_{GT} in the COOLCEP-C is consumed by the CO_2 compressors C2 while only 1% of W_{GT} is consumed by the CO_2 compressors C3 in the COOLCEP-S.
2) The efficiencies η_e and ε are higher for COOLCEP-S than for COOLCEP-C

   In the COOLCEP-S system, the higher turbine backpressure with a higher turbine exhaust temperature makes more heat available for recuperation, this reducing the fuel (natural gas) demand and the specific power output drops too, but the effect of fuel demand drop dominates. As a result, the COOLCEP-S has a thermal efficiency η_e higher by 14.5% than that of the COOLCEP-C.

   One reason of the high efficiency in these systems is the high turbine exhaust heat recuperation with the recuperator effectiveness being above 0.9, while the minimal heat transfer temperature difference is 45 °C. In a gas turbine with a high *TIT* and low pressure ratio, a high recuperator effectiveness of above 0.9 is attainable easily. Also as shown in Ref. [29], it is the heat transfer temperature difference along the recuperator rather than its effectiveness that is the best criterion for gas turbine power cycle recuperator performance evaluation, as it represents the compromise between reducing the temperature difference to improve system exergy losses (and thus increase its efficiency), and the accompanying typical increase in recuperator size and cost. The heat transfer temperature difference chosen value of >45C will not introduce significant difficulties in its design and manufacture.
3) The COOLCEP-S system needs/accommodates a higher cooling LNG mass flow rate.

   Because of the low specific power output in the COOLCEP-S system, generation of the same amount electricity (the power generation capacity is fixed in this comparison at 20 MW), the COOLCEP-S system requires a higher working fluid mass flow rate than that in the COOLCEP-C system, and thus

Table 3
Cycle performance summary.

	COOLCEP-S	COOLCEP-C
Net power output, W_{net} [MW]	20	20
CO_2 condensation pressure [bar]	7/60[a]	7/60[a]
Turbine backpressure p_b [bar]	7.1	1.1
Combustor outlet temperature and pressure [°C/bar]	900/28	900/28
Turbine outlet temperature [°C]	701	474
LNG mass flow rate m_{LNG} [kg/s]	95.16	61.8
Fuel mass flow rate m_f [kg/s]	0.69	0.79
Main working fluid mass flow rate [kg/s]	101.6	60.45
Power consumption in ASU [MW]	2.33	2.67
Specific power output W_{sp} [kJ/kg]	197	332
Refrigeration output, Q_c [MW]	56.7	26.6
Refrigeration exergy, E_C [MW]	8.90	4.09
Ratio of power/cooling energy, R	2.25	4.91
Thermal efficiency, η_e [%]	59.1	51.6
Exergy efficiency, ϵ [%]	39.8	37.3

[a] 7 Bar is the condensation pressure for the main working fluid in the condenser; and 60 bar is the condensation pressure for a small fraction of the working fluid (stream 16).

Table 4
The stream parameters of the COOLCEP-S cycle.

Stream no.	T (°C)	p (bar)	m (kg/s)	Vapor fraction	Molar composition (%)								
					N_2	O_2	CH_4	C_2H_6	C_3H_8	C_4H_{10}	H_2O	CO_2	AR
1	−50.1	6.97	101.61	0	0	0	0	0	0	0	0	99.8	0.2
2	−49.5	29.68	101.61	0	0	0	0	0	0	0	0	99.8	0.2
3	8	29.4	101.61	1	0	0	0	0	0	0	0	99.8	0.2
6	15.5	29.12	104.49	1	0.1	3.6	0	0	0	0	0	96	0.3
7	656.4	28.84	104.49	1	0.1	3.6	0	0	0	0	0	96	0.3
8	8	70	0.688	1	0.3	0	90.8	5	2.9	1	0	0	0
9	900	28	105.17	1	0.1	0.1	0	0	0	0	3.3	96.2	0.3
10	701.4	7.15	105.17	1	0.1	0.1	0	0	0	0	3.3	96.2	0.3
11	65.2	7.13	105.17	1	0.1	0.1	0	0	0	0	3.3	96.2	0.3
13	0	7.1	103.68	1	0.1	0.1	0	0	0	0	0	99.5	0.3
14	−50	7	103.68	0.02	0.1	0.1	0	0	0	0	0	99.5	0.3
15	−50.1	6.97	2.06	1	3.9	1.6	0	0	0	0	0	88.8	5.6
17	−34.9	60	2.06	0	3.9	1.6	0	0	0	0	0	88.8	5.6
18	−161.5	1.01	95.16	0	0.3	0	90.8	5	2.9	1	0	0	0
20	−49.8	72.1	95.16	0.928	0.3	0	90.8	5	2.9	1	0	0	0
21	−34.2	71.4	95.16	1	0.3	0	90.8	5	2.9	1	0	0	0

correspondingly a larger LNG mass flow rate is needed (or accommodated, considering the objective of LNG evaporation for ultimate distribution by the terminal) for the cycle heat rejection process. As a result, the COOLCEP-S system also produces more cooling from the evaporation of the working fluid and the cooling/evaporating LNG. The produced cooling temperature profile in EVA1 in COOLCEP-S is shown in Fig. 11. The refrigeration capacity in EVA1 is about 42.4 MW, out of which more than 95% (40.6 MW) is produced at temperatures between −50 °C and −6 °C, and the LNG heating in HEX3 can add 14.5 MW cooling capacity in a temperature region of −35 °C to 8 °C. This information also allows matching of the produced refrigeration with potential commercial need for it.

The exergy efficiency ε, which takes into accounts both power generation and refrigeration production as commercially useful outputs, is 6.6% higher in the COOLCEP-S than in the COOLCEP-C.

4) Preliminary economic analysis: the COOLCEP-S system has a shorter payback period

The preliminary economic analysis was based on the following assumptions.

- The CO_2 credit price is assumed as 25 EUR/ton.
- The electricity price is 0.045 EUR/kWh.
- The price of natural gas from LNG is 0.15 EUR/Nm^3 for power generation in China.
- The coldness energy of LNG is free, and we need not pay for it.
- The annual running time is 7000 h per year, and the plant life is 20 years. The construction period is 2 years.
- The interest rate is 8%.
- 50% of total investment cost is an interest-bearing loan, and the loan period (years) which is assumed to be equal to the system life.

Balance of plant (BOP) consists of the remaining systems, components, and structures that comprise a complete power plant or energy system that is not included in the prime mover [30]. As the systems are more complex than the conventional power generation system, here we assumed that the BOP account for 20% of the known component cost of the system.

The term O&M is the cost of operating and maintenance, assumed to be 4% of the first cost of the system [31]. Taxes and insurance are not considered in this preliminary evaluation.

The investment estimation of the two systems is listed in Table 6. From Table 6 we can find that the investment cost for the COOLCEP-S system is about 750 EUR/kWe, which is 5.6% lower than that for the COOLCEP-C system. Table 7 presents the economic

Table 5
The stream parameters of the COOLCEP-C cycle.

Stream no.	T (°C)	p (bar)	m (kg/s)	Vapor fraction	Molar composition (%)								
					N_2	O_2	CH_4	C_2H_6	C_3H_8	C_4H_{10}	H_2O	CO_2	AR
1	−50.1	6.95	60.45	0	0	0	0	0	0	0	0	99.8	0.2
2	−49.5	29.68	60.45	0	0	0	0	0	0	0	0	99.8	0.2
3	8	29.4	60.45	1	0	0	0	0	0	0	0	99.8	0.2
6	22.9	29.12	63.74	1	0.2	6.6	0	0	0	0	0	92.8	0.4
7	428.9	28.84	63.74	1	0.2	6.6	0	0	0	0	0	92.8	0.4
8	8	70	0.789	1	0.3	0	90.8	5	2.9	1	0	0	0
9	900	28	64.53	1	0.2	0.1	0	0	0	0	6.1	93.2	0.4
10	473.9	1.08	64.53	1	0.2	0.1	0	0	0	0	6.1	93.2	0.4
11	70.2	1.06	64.53	1	0.2	0.1	0	0	0	0	6.1	93.2	0.4
13	0	1.03	62.85	1	0.2	0.1	0	0	0	0	0	99.3	0.4
13a	75.1	7.1	62.85	1	0.2	0.1	0	0	0	0	0	99.3	0.4
14	−50	7	62.85	0.038	0.2	0.1	0	0	0	0	0	99.3	0.4
15	−50.1	6.95	2.38	1	3.9	1.6	0	0	0	0	0	88.9	5.6
17	−35.8	60	2.38	0	3.9	1.6	0	0	0	0	0	88.9	5.6
18	−161.5	1.01	61.8	0	0.3	0	90.8	5	2.9	1	0	0	0
20	−33.7	72.1	61.8	1	0.3	0	90.8	5	2.9	1	0	0	0
21	1	71.4	61.8	1	0.3	0	90.8	5	2.9	1	0	0	0

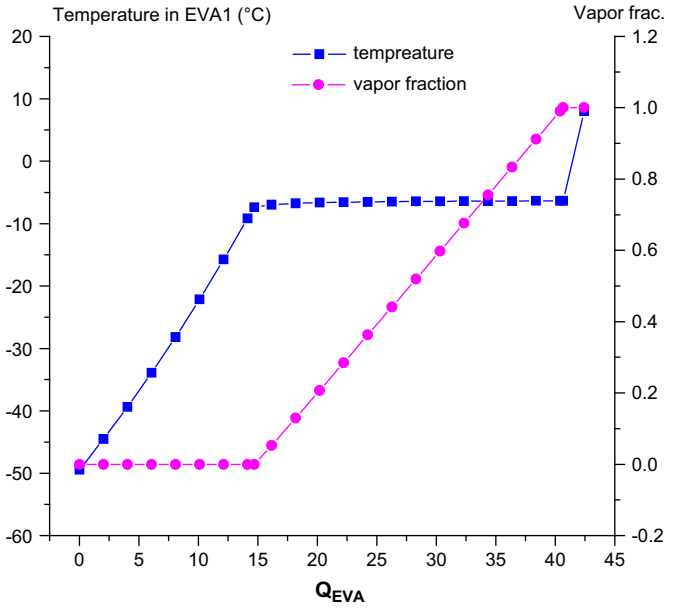

Fig. 11. The temperature profile of the produced refrigeration in EVA1 in the COOLCEP-S system.

analysis results. The payback period is calculated with the consideration of interest rate and the 2 years construction period. The cost of electricity in the operation period is calculated as:

$$COE = \frac{\beta C_i + C_m + C_f - C_{CO_2}}{H \cdot W_{net}} \quad (4)$$

C_i is the total plant investment, C_m is the annual O&M cost, C_f is the annual fuel cost, and C_{CO_2} is the annual CO_2 credit. The refrigeration profit should be taken into account if there is a market for the produced refrigeration. H is the annual operation hours. β is a function of interest rate and the plant operation life n:

$$\beta = i/\left[1-(1+i)^{-n}\right] \quad (5)$$

with $n = 20$, $i = 8\%$, and $\beta = 0.1019$.

The above estimation is based on the assumption that there is no market for the refrigeration. If the refrigeration can also be sold, the payback time will be shortened remarkably, by 2–3 years.

Table 6
Investment cost of the two systems.

Items (10^3 EUR)	COOLCEP-S	COOLCEP-C
Air separation unit	3160	3620
Oxygen compressor	360	400
Gas turbine	5800	6800
Recuperator	2000	500
CO_2 condenser CON	250	170
Exhaust gas compressors C3	260	280
LNG pump	250	200
Low temperature heat exchangers	100	80
Second CO_2 condenser HEX2	50	50
CO_2 compressor C2	–	1000
LNG evaporator with seawater (standby)	300	180
BOP	2506	2656
Total plant cost	15,036	15,936
Specific cost (EUR/kWe)	751.8	796.8

Table 7
Economic analysis results.

	COOLCEP-S	COOLCEP-C
Annual operation hours	7000	7000
Electricity output (10^6 kWh/yr)	140	140
CO_2 recovery (10^3 tons/yr)	47.4	55
Natural gas consumption (10^6 Nm^3/yr)	21.6	24.7
LNG evaporation (10^6 tons/yr)	2.4	1.56
Investment cost (10^6 EUR)	15.036	15.936
Construction interest (10^6 EUR)	1.251	1.326
Total plant investment C_i (10^6 EUR)	16.287	17.262
Income from produced electricity (10^6 EUR/yr)	6.3	6.3
CO_2 credit C_{CO_2} (10^6 EUR/yr)	1.186	1.376
Cost of fuel C_f (10^6 EUR/yr)	3.234	3.706
O&M C_m (10^6 EUR/yr)	0.601	0.637
Payback period (years)	7.74	8.95
COE (EUR/kWh)	0.031	0.034

The two systems are economically competitive having a payback period that is shorter than that of conventional plants, and are thus considered to be feasible and attractive for Chinese LNG stations.

A more detailed thermoeconomic and sensitivity analysis was recently performed by the authors [32].

5) Both systems can accomplish high CO_2 capture

The combustion-generated CO_2 recovery ratios are nearly 100% for both systems. The recovered CO_2 stream is in the liquid state, and is a mixture of 88% CO_2, 2% O_2, 4% N_2 and 6% Ar by volume. Further purification might be required to remove some components prior to transportation and storage, and would add to the overall cost [27].

6. Concluding remarks

Two of the COOLCEP power system configurations with LNG coldness exergy utilization and CO_2 capture are proposed, simulated and compared. These systems feature a high heat addition temperature level with high turbine inlet temperature and turbine exhaust heat recuperation, and a heat sink at a temperature lower than the ambient accomplished by heat exchange with LNG, and thus offer high power generation efficiency. These low temperatures also allow condensation of the working fluid and the combustion-generated CO_2 is thus captured. Furthermore, the subcritical re-evaporation of the CO_2 working fluid is accomplished below ambient temperature and can thus provide refrigeration if needed.

It is found that the COOLCEP-S configuration has higher power generation efficiency, and the COOLCEP-C configuration has high specific power output. Both systems were found to have high thermal performance and low environment impact.

The influence of the turbine inlet temperature *TIT*, the turbine blade cooling, and the turbine backpressure was investigated.

It was decided to drop the turbine inlet temperature *TIT* from 1250 °C to 900 °C to eliminate the need for turbine blade cooling and for advanced gas turbines with the associated technology difficulties and cost. Reduction of the *TIT* also lowers the turbine exhaust temperature *TOT*, thus avoiding the technological difficulties and high cost of the high temperature recuperator.

The operation difference between the two systems is the turbine backpressure. Turbine blade cooling has a higher detrimental effect on the efficiency of the COOLCEP-S system that has a higher turbine backpressure and exit temperature, because the working fluid exhausts at the turbine exit is at a higher temperature, and therefore most of the expansion passage in the turbine needs to be

cooled. In the COOLCEP-C system the passage portion that must be cooled is by the same token smaller. Without blade cooling, the system efficiency increases with the increase of the backpressure in the low backpressure region. This makes the COOLCEP-S configuration attractive when the turbine blades aren't cooled.

With *TIT* at 900 °C, the COOLCEP-C configuration has a specific power output of 330 kJ/kg, and a power generation efficiency of 51.6%. The COOLCEP-S configuration has a specific power output of 197 kg/kg, which is lower by 40% compared with that of the COOLCEP-C configuration, but it is noteworthy that this value is still comparable or even higher than the specific power output of commercial gas turbines with the same *TIT* value. The COOLCEP-S system has a much higher power generation efficiency of 59.1% as the pressure evaluation is by pump work. Both configurations have a high CO_2 capture ratio.

A preliminary economic evaluation has also been performed and explained in detail in Ref. [32]. This was done by extensive sensitivity analyses of the cost of produced electricity with and without saleable refrigeration to the pressure ratio, *TIT*, and major heat exchanger temperature differences, which resulted in an economically optimized plant. The capital investment cost of such a plant is about 750–800 EUR/kWe and the payback period is about 8–9 years including the construction period, both better than those of the latest conventional fossil fuel power plants built in China that do not even separate CO_2, and the cost of electricity is estimated to be 0.031–0.034 EUR/kWh.

Acknowledgement

The authors gratefully acknowledge the support from the Statoil ASA, and the Chinese Natural Science Foundation Project (No. 50520140517). We would also like to express our great appreciation to Messrs. Geir Johan Rortveit, Bengt Olav Neeraas, Jostein Pettersen, Gang Xu and Hu Lin for their very valuable comments and discussion.

Appendix

Gas turbine cooling model

A discrete (rather than differential field) model was used to analyze the blade cooling and its effects because it is computationally more convenient. As shown in Fig. A1, in such a discrete model we reduced the expansion path into a number of discrete elementary operations, in which the gas expansion process in the turbine includes several mixing processes between the expanding hot gas and the fluid streams added for blade cooling. It considers the turbine stage-by-stage, and estimates the cooling flow necessary for the stator and rotor of each stage. The stator flow is assumed to mix with the main gas flow prior to flow through the turbine, i.e., the mixing happens before the power extraction. The rotor coolant flow is mixed into the main stream at the rotor exit (after the power extraction).

For each cooling step, the required coolant mass flow is calculated using [33–35]:

$$\frac{m_c}{m_g} = \frac{C_{pg}}{C_{pc}} St_g \frac{A_b}{A_g} \frac{1}{\eta_c} \frac{\varepsilon_c}{1-\varepsilon_c}\left(1-\delta_f\right) \tag{A1}$$

where subscripts g and c refer to the main gas stream and the cooling stream, respectively. St_g is main gas Stanton number, A_b is the blade surface area, A_g is the flue gas path cross-sectional area, and η_c is the cooling efficiency.

The cooling effectiveness ε_c is defined as:

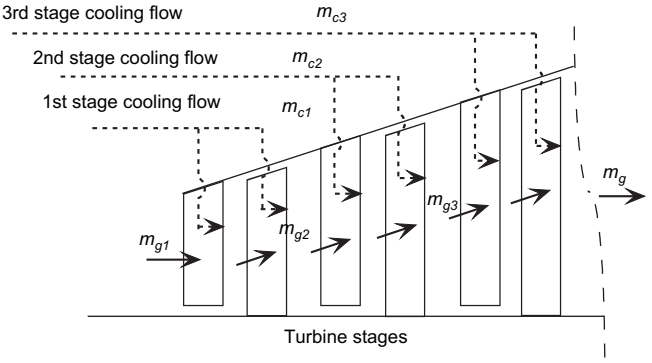

Fig. A1. Schematic diagram of the turbine blade cooling model.

$$\varepsilon_c = (T_g - T_b)/(T_g - T_c) \tag{A2}$$

For an advanced gas turbine generation, commonly used values for St_g, A_b/A_g and η_c are 0.005, 4 and 0.3, respectively [36]. T_b refers to the turbine blade metal temperature; its typical value is 1123 K (850 °C) and is kept constant in the calculation.

Comparing with internal convection cooling, the cooling flow rate requirement is reduced by more than 40% if film cooling is employed. The film cooling effectiveness δ_f is adopted in the present study to account for this difference. $\delta_f = 0.47$ for film cooling, and $\delta_f = 0$ in case of simply convective cooling with no film [37].

The pressure loss due to the mixing of the coolant with the gas was set as proportional to the ratio between the local coolant mass flow and the corresponding main gas mass flow [37]:

$$\Delta p_{mix,i} = p_{g,i} \cdot m_{c,i}/m_{g,i} \tag{A3}$$

For the oxy-fuel systems proposed and analyzed in this study, the coolant for the blade cooling is extracted continuously from the working fluid in the recuperator REP, the extracted stream is the recycled CO_2 stream at the state of 200 °C/29 bar.

The cooled stages are divided based on the expansion profile of COOLCEP-C because of its full expansion. The turbine in COOLCEP-C is divided into 4 stages assuming equal enthalpy drops. Once the mixing point pressures are determined, they are fixed regardless of the variation of the turbine backpressure, which means that in COOLCEP-S, the dividing point of each stage is the same as that in COOLCEP-C. This assumption is based on the fact that they share the same temperature profile in the higher pressure expansion where blade cooling is employed. Starting from the first stage, the turbine cooling model (Eqs. (A1)–(A3)) has been applied to determine the coolant ratio for each stator and rotor, until the working gas reached the allowed metal blade temperature T_b, thus dividing the expansion passage into cooled part and uncooled part. The uncooled part shrinks as the turbine backpressure increases; the turbine in COOLCEP-S is almost all the cooled part.

It is noteworthy that in this study we assume that film cooling is used for the blades. If more advanced cooling, such as transpiration blade cooling, would be used, the efficiency loss would be much lower than we calculate here.

References

[1] Karashima N, Akutsu T. Development of LNG cryogenic power generation plant. In: Proceedings of 17th IECEC; 1982. p. 399–404.
[2] Angelino G. The use of liquid natural gas as heat sink for power cycles. ASME Journal of Engineering for Power 1978;100:169–77.
[3] Kim CW, Chang SD, Ro ST. Analysis of the power cycle utilizing the cold energy of LNG. International Journal of Energy Research 1995;19:741–9.

[4] Najjar YSH, Zaamout MS. Cryogenic power conversion with regasification of LNG in a gas turbine plant. Energy Conversion and Management 1993;34:273–80.
[5] Wong W. LNG power recovery. Proceedings of the Institution of Mechanical Engineers, Part A: Journal of Power and Energy 1994;208:1–12.
[6] Deng S, Jin H, Cai R, Lin R. Novel cogeneration power system with liquefied natural gas (LNG) cryogenic exergy utilization. Energy 2004;29:497–512.
[7] Krey G. Utilization of the cold by LNG vaporization with closed-cycle gas turbine. ASME Journal of Engineering for Power 1980;102:225–30.
[8] Agazzani A, Massardo AF. An assessment of the performance of closed cycles with and without heat rejection at cryogenic temperatures. ASME Journal of Engineering for Gas Turbines and Power 1999;121:458–65.
[9] Chiesa P. LNG receiving terminal associated with gas cycle power plants. ASME paper 97-GT-441; 1997.
[10] Desideri U, Belli C. Assessment of LNG regasification systems with cogeneration. In: Proceedings of TurboExpo 2000; 2000. Munich, Germany, 2000-GT-0165.
[11] Kim TS, Ro ST. Power augmentation of combined cycle power plants using cold energy of liquefied natural gas. Energy 2000;25:841–56.
[12] Riemer P. Greenhouse gas mitigation technologies, an overview of the CO_2 capture, storage and future activities of the IEA greenhouse gas R&D program. Energy Conversion and Management 1996;37:665–70.
[13] Haugen HA, Eide LI. CO_2 capture and disposal: the realism of large scale scenarios. Energy Conversion and Management 1996;37:1061–6.
[14] Jericha H, Gottlich E, Sanz W, Heitmeir F. Design optimization of the Graz cycle prototype plant. ASME Journal of Engineering for Gas Turbines and Power 2004;126:733–40.
[15] Sanz W, Jericha H, Moser M, Heitmeir F. Thermodynamic and economic investigation of an improved Graz cycle power plant for CO_2 capture. Journal of Engineering for Gas Turbines and Power 2005;127:765–72.
[16] Anderson R, Brandt H, Doyle S, Pronske K, Viteri F. Power generation with 100% carbon capture and sequestration. Second annual conference on carbon sequestration, Alexandria, VA; 2003.
[17] Marin O, Bourhis Y, Perrin N, Zanno PD, Viteri F, Anderson R. High efficiency, zero emission power generation based on a high-temperature steam cycle. 28th International technical conference on coal utilization & fuel systems, Clearwater, FL, USA; 2003.
[18] Mathieu P, Nihart R. Zero-emission MATIANT cycle. Journal of Engineering for Gas Turbines and Power 1999;121:116–20.
[19] Mathieu P, Nihart R. Sensitivity analysis of the MATIANT cycle. Energy Conversion and Management 1999;40:1687–700.
[20] Zhang N, Lior N. A novel near-zero CO_2 emission thermal cycle with LNG cryogenic exergy utilization. Energy 2006;31:1666–79.
[21] Zhang N, Lior N. Proposal and analysis of a novel zero CO_2 emission cycle with liquid natural gas cryogenic exergy utilization. Journal of Engineering for Gas Turbine and Power 2006;128:81–91.
[22] Ishida M, Jin H. CO_2 recovery in a novel power plant system with chemical-looping combustion. Energy Conversion and Management 1997;38(19):187–92.
[23] Ishida M, Jin H. A new advanced power-generation system using chemical-looping combustion. Energy – The International Journal 1994;19:415–22.
[24] Griffin T, Sundkvist SG, Asen K, Bruun T. Advanced zero emissions gas turbine power plant. ASME Journal of Engineering for Gas Turbines and Power 2005;27:81–5.
[25] Kvamsdal HM, Jordal K, Bolland O. A quantitative comparison of gas turbine cycles with CO_2 capture. Energy 2007;32:10–24.
[26] Aspen Plus®, Aspen Technology, Inc., Version 11.1, http://www.aspentech.com/.
[27] Davison J. Performance and cost of power plants with capture and storage of CO_2. Energy 2007;32:1163–76.
[28] Lior N, Zhang N. Energy, exergy, and second law performance criteria. Energy – The International Journal 2007;32:281–96.
[29] Cai R. A new analysis of recuperative gas turbine cycles. Proceedings of the Institution of Mechanical Engineers, Part A: Journal of Power and Energy 1998;212(4):289–96.
[30] Larson ED, Ren T. Synthetic fuel production by indirect coal liquefaction. Energy for Sustainable Development 2003;VII(4).
[31] Kreutz T, Williams R, Consonni S, Chiesa P. Co-production of hydrogen, electricity and CO_2 from coal with commercially ready technology. Part B: economic analysis. Hydrogen Energy 2005;30:769–84.
[32] Liu M, Lior N, Zhang N, Han W. Thermoeconomic optimization of COOLCEP-S: a novel zero-CO_2-emission power cycle using LNG (liquefied natural gas) coldness. Paper IMECE2008-66467, Proceedings of IMECE2008, 2008 ASME international mechanical engineering congress and exposition, October 31–November 6, 2008, Boston, Massachusetts, USA.
[33] Stecco S, Facchini B. A computer model for cooled expansion in gas turbines. Proceedings of the ASME Cogen-Turbo symposium, Nice, France; 1989.
[34] Abdallah H, Harvey S. Thermodynamic analysis of chemically recuperated gas turbines. International Journal of Thermal Sciences 2001;40:372–84.
[35] Jordal K, Bolland O, Klang A. Aspects of cooled gas turbine modeling for the semi-closed O_2/CO_2 cycle with CO_2 capture. ASME Journal of Engineering for Gas Turbines and Power 2004;126:507–15.
[36] Elmasri MA. On thermodynamics of gas turbine cycles: part 2 – a model for expansion in cooled turbines. ASME Journal of Engineering for Gas Turbines and Power 1986;108:151–9.
[37] Fiaschi D, Lombardi L. Cellular thermodynamic model for gas turbine blade cooling. Proceedings of the ECOS 2001, the international efficiency, energy, optimization, simulation and environmental aspects of energy systems and processes symposium, Istanbul, Turkey, June 4–6, 2001.